Appl Nanosci (2016) 6:7–17
DOI 10.1007/s13204-015-0419-5

ORIGINAL ARTICLE

Catalytic oxidation of carbon monoxide over supported palladium nanoparticles

Keshav Chand Soni · R. Krishna · S. Chandra Shekar · Beer Singh

Received: 22 September 2014 / Accepted: 11 February 2015 / Published online: 25 February 2015

Abstract Catalytic oxidation of CO with ozone had been studied over Al_2O_3 and SiO_2 supported Pd nanoparticles which was synthesized by two different methods. The polyol method mainly resulted in highly dispersed Pd particles on the support, while the impregnation method resulted in agglomeration Pd particles on the support. Supported Pd nanoparticles synthesized from $PdCl_2$ in the presence of poly (*N*-vinylpyrrolidone) (PVP) by chemical reduction. The catalysts were characterized by X-ray diffraction, N_2 BET surface area, pore size distributions, CO chemisorption, TEM and H_2-temperature programmed reduction. The physico-chemical properties were well correlated with activity data. Characterizations of XRD and TEM show that the surface Pd nanoparticles are highly dispersed over Al_2O_3 and SiO_2. The catalytic activity was dependent upon ozone/CO ratio, contact times, and the reaction temperature. The extent of carbon monoxide oxidation was proportional to the catalytically ozone decomposition. The PVP synthesized Pd/A_2O_3 catalyst had been found to be highly active for complete CO removal at room temperature. The higher activity of the nanocatalyst was attributed to small particle size and higher dispersion of Pd over support.

Keywords Pd · CO · TPR · Ozone · PVP · Nanoparticles · Catalytic oxidation

K. C. Soni (✉) · R. Krishna · S. Chandra Shekar · B. Singh
Protective Devices Division, Defence R&D Establishment, Jhansi Road, Gwalior 474002, India
e-mail: keshavsoni2k@gmail.com

Introduction

Low temperature catalytic oxidation of CO over the supported nanosized metal catalyst has recently drawn much attention due to its high performance for controlling environmental pollution (Seyfi et al. 2009). The metal oxides catalyst with variable oxidation states of metal ions (Gadgil et al. 1994; Kulshreshtha and Gadgil 1997), or supported noble metals catalysts (Pt, Pd, and Au catalysts) show excellent performance for CO oxidation at low temperature, but its stability is lower and its activity quickly declines with time on stream (Yu et al. 2008, 2009). It is suggested that supported Pd catalysts may be a good alternative to gold in CO oxidation if proper preparation method and support are adopted (Wang et al. 2014).

Catalytic CO oxidation process in the presence of ozone has high pollutant removal efficiency and low energy consumption, which is required for conventional CO removal process (Almquist et al. 2007). The high reaction rates are observed for CO oxidation process over Au/Fe_2O_3, CeO_2, Co–Cr, Pt–Pd, and Mn catalysts, which is due to the decomposition of ozone into the highly reactive oxygen species that can oxidize pollutants (Chang and Sheng 2005; Hao et al. 2001; Soni et al. 2015). Naccache (1971) have been confirmed the formation of surface O^- species during ozone decomposition, which interacts with CO and form a CO_2^- radical species on magnesium oxide surface. Konova et al. (2004) also reported that the formation of catalytically active complex O^- $[Co^{4+}]$ over Co/Al_2O_3 catalyst, which is responsible for complete oxidation of volatile organics. The $Pt–Pd/Al_2O_3$ catalyst provides better efficiency for CO removal than the Mn-loaded catalyst (Chang and Sheng 2005). Catalytic oxidation of

CO over Pt/Al_2O_3 is reported at low temperature and the rate of reaction is very slow in presence of O_2 at the same reaction conditions. The rate of reaction is observed to be proportional to the square root of O_2 partial pressure and independent of CO concentration. On the other hand, in presence of ozone, rapid CO oxidation is observed which is ascribed to the reaction of gaseous ozone directly reacting with surface adsorbed CO by Eley–Rideal mechanism. Ozone decreases the Pt-surface poisoning by CO adsorption at room temperature (Petersson et al. 2006). The CO surface coverage is not significantly affected between the reactions of gaseous ozone with adsorbed CO over Pt/Al_2O_3 catalyst at low ozone concentrations and low reaction temperatures. Attempts have been made to identify the low-temperature catalytic process by highly dispersed gold deposited nanoparticles using air as an oxidant (Konova et al. 2004). Activation energies of 18 and 16 kJ/mol are reported for Au/ZrO_2 and Au/Co_3O_4 nanoparticles, respectively; whereas, 30 kJ/mol is reported for Au/TiO_2 in the temperature range of 220–278 K by Haruta et al. (1993). Konova et al. (2004) confirmed the formation of carbonates and the subsequent blockage of active sites, which are responsible for the loss of catalytic activity over a certain period. Au catalysts are reported as better than Ag and Ni containing catalysts for CO oxidation in presence of ozone (Hao et al. 2001; Haruta and date 2001). Most of the literature reports have been confirmed the formation of superoxide species (O^{2-}) during ozone decomposition over catalytic surface (Almquist et al. 2007; Hao et al. 2001). Amongst the readily available CO oxidation catalysts, Pd-based catalysts have received considerable interest since they are intrinsically more active for CO oxidation (Lashina et al. 2012). It has been reported that relative CO oxidation activities of Pd metal are higher than other metals at 300 °C (Heck and Farrauto 2002). The Pt/Rh catalyst is more active than Pd/Rh under molecular oxygen as an oxidant, whereas Pd/Rh is more active than Pt/Rh when ozone is employed as an oxidant (Chang and Sheng 2005). It is also observed that increasing CO concentration in reaction mixture results in decrease of CO conversion; however, even at higher concentrations of CO, the nanocatalysts still have acceptable destruction ability to oxidize CO (Estifaee et al. 2013).

Recent progress in nanoscience, particularly in colloidal synthetic methods, has enabled the synthesis of metal nanoparticles with precisely controlled size, shape, and composition (Li et al. 2008; Weiliang et al. 2013). A suspension of nanosized catalyst is unstable, which is easy to aggregate and precipitate from the catalytic systems resulting in a decrease of catalytic activity. For preventing the coagulation and precipitation of the metal nanoparticles, a capping agent is required during the formation of nanosized metal catalysts. It is reported that better dispersion of silver nanoparticles is observed when PVP is used as a capping agent with an alcohol under reflux condition (Mulvaney 1996; Lu et al. 1999). Stable colloidal Pd has been prepared by controlling the reduction of $PdCl_2$ reduction time with Pd^{2+} ion concentrations, and reduction temperatures in the presence of PVP. PVP has two hetero atoms (oxygen, nitrogen) which make the capping of metal particles more efficient leading to size reduction of Pd particles (Telkar et al. 2004). Li et al. (2008) have found that Pt/Fe_2O_3 prepared by a colloid-deposition method is relatively more active for CO oxidation under wet conditions. Huang et al. (1996) suggested that a complex is formed between Ag^+ ions and PVP, followed by the reduction of the Ag atoms on the PVP. Sarkar et al. (2005) developed and optimized an effective technique for the better dispersion of very small metal particles using PVP. In particular, porous supports with a large specific surface area also provide a fine dispersion of nanoparticles, leading to high catalytic activity (Gunay and Yildirim 2013; Kugai et al. 2013).

In this study, Pd/Al_2O_3 and Pd/SiO_2 nanocatalysts are prepared using polyol method and conventional are impregnation method. The percentage of Pd loading is maintained at 1 wt % for both methods. The catalytic properties of Pd nanocatalysts prepared polyol process are compared with impregnated Pd catalysts for CO oxidation, using ozone as an oxidizing agent. The aim of study is to investigate the effect of Pd particle size on ozone decomposition and its influence on CO oxidation reaction.

Experimental

Preparation of catalysts

1 % Pd/SiO_2 and 1 % Pd/Al_2O_3 supported nanocatalysts were synthesized as described previously (Nadgeri et al. 2008) by the reduction of the Pd ions with ethanol using poly (N-vinyl pyrrolidone, PVP) as a stabilizer. Palladium sol was prepared from a solution containing 0.134 g $PdCl_2$ (Aldrich, >99 %) in 15 ml of aqueous HCl and 5.448 g of PVP as a stabilizer. After vigorous stirring and reflux conditions, the ratio of ethanol and water (30:70, v/v) were added over a period of 5 h in N_2 atmosphere at 50 °C. The pH of the Pd precursor solution was about 1.4. For depositing the sol on to the support, 6 g SiO_2 (Harshaw, SA, 300 $m^2\ g^{-1}$ BSS) was added to the above solution after stirring for 16 h. The solid catalyst was filtered and washed with distilled water until the filtered solution became free from PVP and chloride ion. The filtrate was oven dried at

120 °C and reduced at 350 °C in H_2. In a similar manner, other Pd nanoparticles were synthesized on γ-Al_2O_3 (Harshaw, SA, 260 m^2 g^{-1} BSS) support. Both nano-catalysts synthesized by pyrrolidone encapsulated having Pd content of 1 wt % and designated as PAN and PSN for alumina and silica supported systems, respectively.

For comparison, the conventional palladium-supported catalysts were prepared by wet impregnation method. The requisite amount $PdCl_2$ was dissolved in aqueous solution of dilute hydrochloric acid solution containing 0.134 g Pd/ml. The required amount of this solution was mixed with 10 g of γ-Al_2O_3 support at ambient temperature, stirred well for 3 h and then evaporated on a water bath. The samples were oven dried for 12 h at 120 °C, calcined at 350 °C for 4 h in N_2. The resulting catalysts were designated as PA for alumina supported catalysts having Pd content of 1 wt %. Similarly, Pd/SiO_2 was also prepared and designated as PS having Pd loading.

Characterization of catalysts

Brunauer–Emmett–Teller (BET) and Barrett–Joyner–Halenda (BJH) methods were used to estimate the BET surface area and pore size distributions, respectively. Nitrogen adsorption–desorption isotherms were obtained using a surface area analyzer (Micromeritics ASAP 2010) at liquid N_2 temperature (−196 °C). Prior to analyses, 0.2 gm of the catalyst samples was loaded into a quartz tube reactor and degassed at 120 °C with a helium purge for 60 min. A five-point nitrogen adsorption isotherm was used to determine the BET surface area of the samples. X-ray diffraction patterns of the reduced catalysts were recorded on a Rigaku Miniflex (M/s. Rigaku Corporation, Japan) X-ray diffractometer using Ni-filtered Cu Kα radiation (λ = 1.5406 Å) with a scan speed of 2° min^{-1} and a scan range of 2°–80° at 30 kV and 50 mA. The amount of loaded Pd metal on the support was determined by inductively coupled plasma spectrometry-atomic emission spectroscopy. Samples for transmission emission spectroscopy (TEM, JEM-200FX electron microscope) were prepared by keeping a drop of the colloidal solution prepared in acetone as solvent on a copper grid, coated with a thin carbon film. Samples were dried and kept in vacuum oven in a desiccator. Samples for TEM temperature-programmed reduction (TPR) was performed on Nuchrom unit to determine the extent of reducibility of the Pd catalysts. TPR studies on the catalyst samples (0.1 g) were carried out using a 5.6 % H_2–Ar mixture (40 cc/min) in the temperature range 30–600 °C at a heating rate of 10 °C/min. Pulse chemisorption was performed on Newchrom Technologies sorption unit by pulsing CO over the reduced catalyst at room temperature, assuming a chemisorption stoichiometry of 1:1 between CO and Pd (Babu et al. 2007). The palladium dispersion, metal surface area and particle size of the catalysts were calculated using Padmasri et al.'s procedure (2002). Prior to CO pulse chemisorption experiments, the catalyst was reduced in H_2 flow (40 cc/min) at 350 °C for 4 h.

Catalytic experiments

Catalytic activity measurements were carried out in a continuous flow, fixed-bed reactor at atmospheric pressure. For CO oxidation, a quartz reactor packed with 1 g of catalyst (reduced at 350 °C and cooled in N_2 and exposed to air at room temperature) pellet diluted with 0.5 g of glass beads (volume of catalyst bed = 4.5 cm^3) in the middle of the reactor. The reactor had facility to measure the catalyst bed and furnace skin temperature independently. The CO reaction mixture consists of 50 ml/min CO, 100 ml/min O_2, diluted in N_2 with a total gas flow rate of 300 ml min. The flow rates of reaction mixture were adjusted using mass flow controllers (Sierra Instruments Inc, flow accuracy ±1 %). A temperature rise was observed in the catalyst bed as soon as the reaction mixture was passed through the catalytic bed due to the exothermic nature of the oxidation reaction. Hence, a supplemental air flow was used over the reactor outer surface as an external cooling to maintain the constant reaction temperature. The reaction was studied in the temperature range of 30–120 °C, with contact times (τ) from 0.2 to 1.2 s and the ozone to CO mole ratio were varied between 2.5 and 4.5. The exit gas composition was analyzed using calibrated CO and CO_2 analyzers (Technovation Instruments CO-MP94 and CO_2-P89) which were capable of measuring concentrations of CO and CO_2, respectively. Carbon monoxide (Bhuruka Gas Ltd, UHP grade, 9350 ppm in N_2) was used for the reaction. Compressed O_2 cylinder (99.7 % dried over silica gel) was used for the catalytic reactions as well as for the ozone generator. The ozone generator was standardized by the iodometric method (Richard 1993).

Results and discussion

BET-surface area and pore size distribution

Table 1 presents the BET surface area of impregnated and PVP-synthesized Pd reduced catalysts. BET surface areas of supported Pd catalysts are less than that of the original support due to pore blockages of metal particles during impregnation. BET surface areas of the PAN catalyst (224 m^2 g^{-1}) are little higher than PA (200 m^2 g^{-1}) conventional catalyst. On the other hand, surface area of PSN catalyst (205 m^2 g^{-1}) is much higher compare to PS catalyst (162 m^2 g^{-1}). Bumajdad et al. (2006) also reported that decrease in BET surface area is due to sintering as well

Table 1 Catalysts characteristics of supported Pd catalysts

Catalyst code	Pd wt% (ICP)	BET-SA (m^2 g^{-1})	CO uptake (μ mol g^{-1})	D_{co} (%)	MSA m^2/g	PS (nm)	TEM (nm)
PS	0.89	162	6	7.2	0.28	16.5	18
PA	0.86	200	8	9.9	0.38	11.9	14
PSN	0.82	205	14	18.2	0.66	6.5	6
PAN	0.85	224	19	23.8	0.91	4.9	3

D_{CO} % dispersion of Pd, *PS* particle size of Pd, *MSA* metal surface area

as agglomeration of the particles. The high surface area of the catalyst is a very important requirement and it results in more adsorption sites for carbon monoxide to be oxidized. Pore size distributions of the reduced catalyst samples are calculated by BJH desorption equation which suggest the presence of mostly mesopores and macrospores. Figure 1 indicates that average pore size distribution of the PAN and PSN catalysts is 4 and 7 nm, respectively. Rather, PA and PS catalysts average pore size are 5.5 and 7.5 nm, respectively. These small pores may be generated due to burning off the PVP at 350 °C during calcinations (Chou and Chen 2007). The surface area values are decreased more in PA catalyst compared to that of PAN. However, both the values are less than that of Al_2O_3 support. In contrast, the BET surface area values show more decrease in silica catalysts compared to the alumina catalysts. It is due to the fact that the mesopores available in silica are relatively wider and the PVP-stabilized Pd particle might be accessible for the mesopores. Hence the reduction in the BET-SA is more pronounced in case of PSN catalyst as the majority of the silica surface area is contributed by mesopores.

X-ray diffraction

The XRD patterns of reduced Pd supported catalysts depicted in Fig. 2a. The XRD patterns of reduced Pd catalysts samples exhibited the amorphous nature of alumina and crystalline nature of silica. The XRD patterns of the impregnated catalysts (PS and PA), the diffraction signals at $2\theta = 40°$, 46.1°, and 68.2° belonging to the (111) (200) and (220) crystallographic planes of Pd (0) metal, respectively. In the PVP-synthesized catalysts (PAN and PSN), very low intense diffraction signals are observed at $2\theta = 40°$ and 45.9° compared to that of impregnated Pd catalysts. These diffraction signals (at $2\theta = 40°$) are consistent with a characteristic signals of face centered cubic (FCC) metallic palladium (ICDD 46–1043). The peak broadening is also consistent with the nanoscale structural

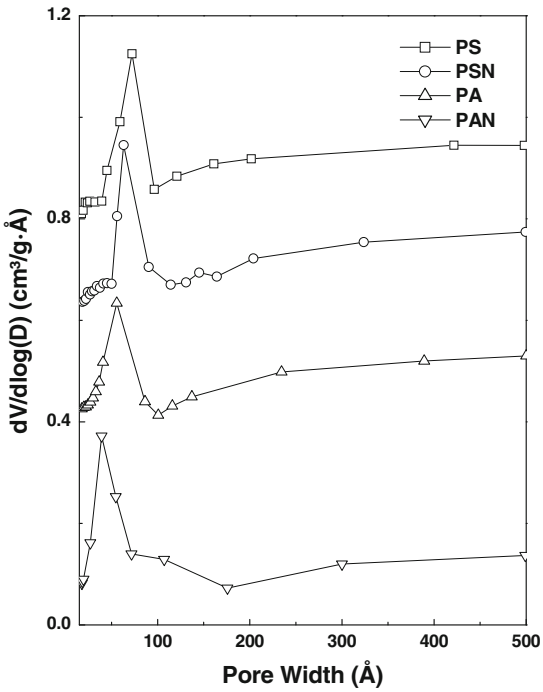

Fig. 1 Pore size distributions of Pd/Al_2O_3 and Pd/SiO_2 catalysts

features of the Pd nanocrystals (Berger et al. 2010). It is observed that in PVP-stabilized nanoparticles, the agglomeration of Pd particle is prevented under reduction condition and the Pd metal particles are finely dispersed on support (Nadgeri et al. 2008).

Temperature programmed reduction

The reducibility of these Pd supported catalysts is determined by temperature-programmed reduction (TPR) experiments. TPR profiles of palladium supported catalysts are shown in Fig. 2b. In impregnated catalysts, a negative peak is observed around at 84 °C (PA) and 76 °C (PS), which is attributed to the formation of β-PdH_x (Chandra Shekar et al. 2003). The shifting of β-PdH_x peak to the lower temperature is observed for PVP synthesized Pd catalysts which are centered at 75 °C (PAN) and 72 °C (PSN). In impregnated catalyst, the peak area of β-PdH_x is higher compared to the PVP-synthesized catalyst, which is attributed to the lower Pd dispersion in the catalyst. Berger et al. (2010) have reported that the formation of β-PdH_x is associated with the presence of larger Pd particles. However, it is observed that the β-PdH_x phase is rarely formed for very small particles, hence a dramatic size reduction in case of PVP synthesized Pd nanocluster could lead to the enhanced catalytic activity. The peak broadening in alumina supported catalysts could be due the formation of metallic Pd nanoparticles with narrow size distribution.

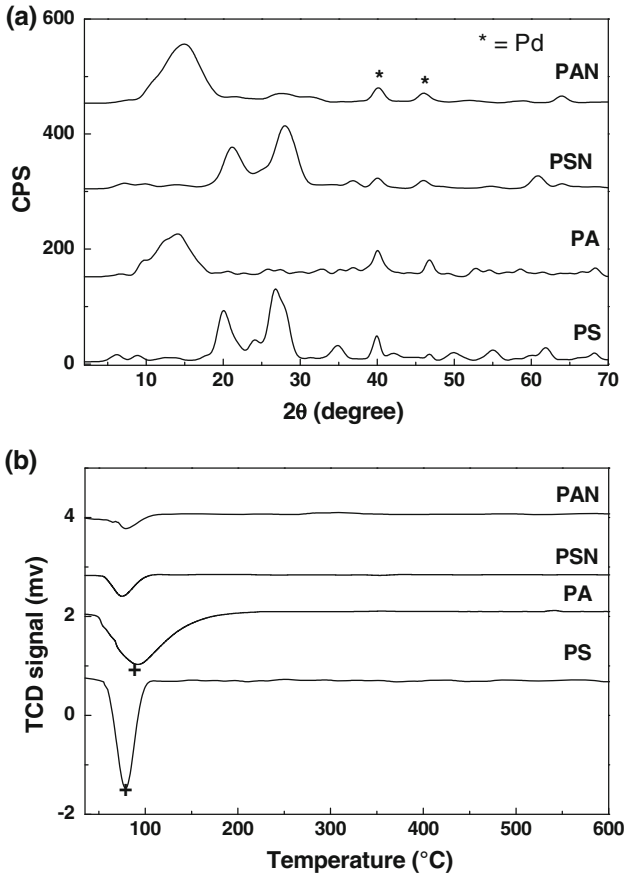

Fig. 2 **a** X-ray diffraction patterns of reduced Pd/Al_2O_3 and Pd/SiO_2 catalysts. **b** Temperature programmed reduction of Pd/alumina and Pd/silica catalysts

CO pulse-chemisorption

The CO-uptakes of the catalysts measured by pulse chemisorption method and found to be maximum for PVP synthesized catalysts and minimum for impregnated catalysts as presented in Table 1. The CO chemisorption studies showed that the metal dispersion found higher for the PSN (18.2 %) and PAN (23.8 %) catalyst as compared to the PA and PS, i.e., 9.9 and 7.2 %, respectively. It is also noted that the dispersion of the particles over the silica support is relatively poor as compared with alumina. This confirms the advantage of the PVP stabilized chemical reduction method over the conventional impregnation method. The percentage dispersion of Pd calculated from the uptakes show that PAN catalyst has exhibited higher CO uptake compared to that of PSN catalyst. The relative dispersion of Pd is higher over PAN compared to PA catalyst, which is attributed to the formation of smaller particles of Pd over this catalyst. This observation is also well supported by the TEM analysis. In case of PAN and PSN catalyst, an increase in CO uptake for nano catalyst also indicated the formation of PVP capped Pd nanoparticles. PVP has a polycationic nature due to the presence of quaternary nitrogen, which helps in stabilizing the Pd nuclei formed during the reduction. The interaction between the negative charge of oxygen on a support surface (Al_2O_3 or SiO_2) and the cationic PVP causes the polymer to occupy the adsorption sites on the support (Toebes et al. 2001). This significant enhancement of CO oxidation activity of supported Pd nanoparticles is mainly due to the small particle size and high dispersion of Pd over support. The nanosized Pd particles are protected by the bulky polymer groups of the stabilizer PVP on the surface PAN and PSN catalyst which can not penetrate through the pores of the support; whereas, in the case of PA and PS catalyst, Pd is adsorbed in several ways including the micropores of the support and such sites would be inaccessible for catalytic reaction (Simonov et al. 1997). This phenomenon also reflected in the pore size distributions and BET surface area values.

TEM analysis

Figure 3 shows the TEM images of the sample after the deposition of Pd sol on the Al_2O_3 and SiO_2 support. The figure clearly shows that the palladium particles are well dispersed on the support. It is clear from the TEM images that Pd species are homogeneously dispersed on the supports and the particle sizes are mainly between 3 and 18 nm. TEM results indicate that the Pd particle size of PVP-synthesized catalysts become much smaller compared with impregnated samples. It is found that the formed Pd nanoparticles are more uniformly dispersed over the Al_2O_3 support for PAN catalyst (Fig. 3a), and small Pd nanoparticles with narrow size distribution are also observed.

In the PVP-stabilized Pd colloidal system, a strong interaction between C=O groups of PVP and Pd metal are formed, which results in the small size of the Pd nanoparticles (Hirai et al. 1985). The particle sizes of Pd strongly depend on the Pd–PVP interaction which prevents the aggregation of Pd nanoparticles. It would be beneficial for the formation of uniformly dispersed Pd nanoparticles, their stability and catalytic properties.

Figure 4 shows the histogram of the particle size distributions as calculated from the TEM images of the PVP synthesized as well as impregnated Pd catalysts. In PAN catalyst, 65 % of the particles are in range of 2–6 nm. In contrast, 52 % of the particles in the impregnated catalysts observed to be in the range of 10–14 nm. The Pd nano particles obtained in this study are comparable with 6.3 nm for Pd catalysts which were prepared by Berger et al. (2010). Lim et al. (2007) reported that PVP is strongly

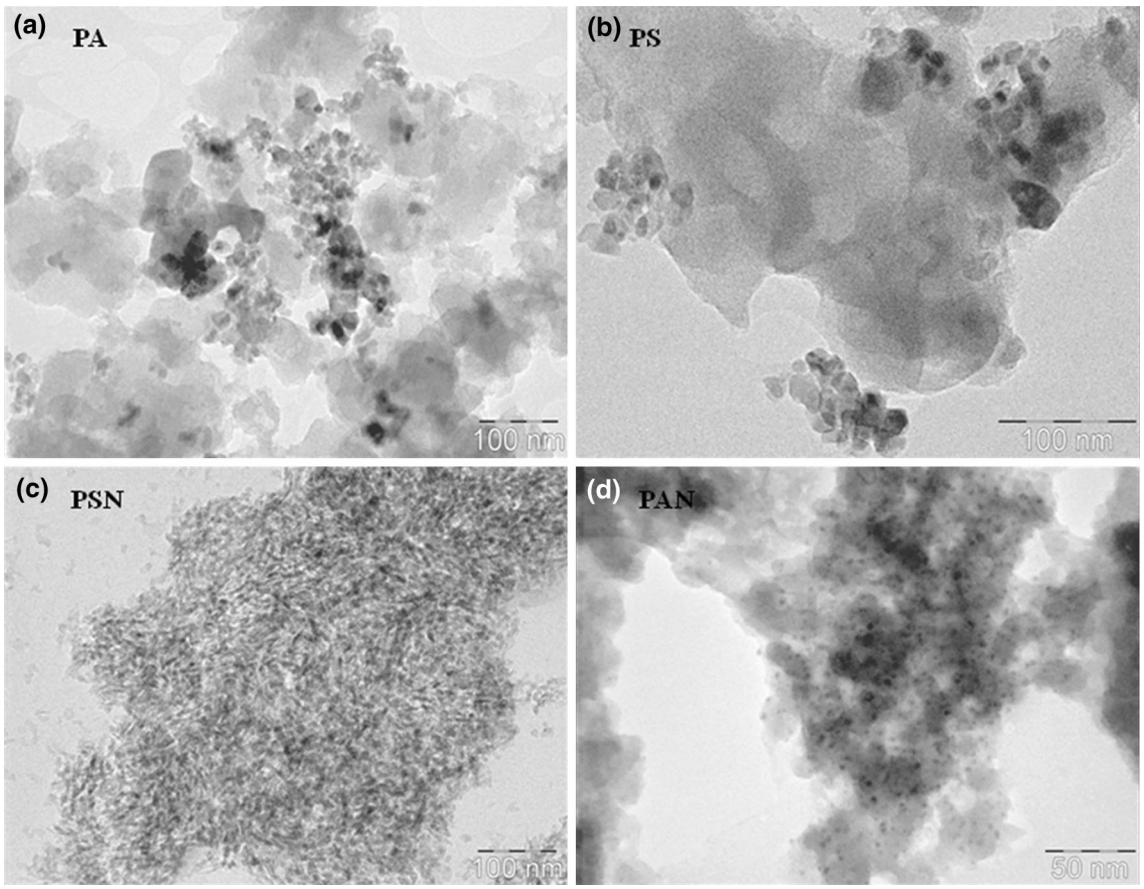

Fig. 3 TEM micrographs of Pd/alumina supported catalysts. **a** PA, **b** PS, **c** PAN, **d** PSN

bound to the (100) facets of Pd and affect the relative growth rates of different facets, this might be favored for multi-twinned particles. The sponge-like structure is also reported with high magnification micrograph, which is built up by primary nanoparticles with an average dimension of 5 nm (Shen et al. 2009). It appears that these small primary nanoparticles are interconnected with one another to form larger secondary spherical sponge-like architectures with recognizable boundaries or voids between the component subunits. The Pd particle sizes measured from the TEM are very similar with the result obtained from XRD by Shen et al. (2009). It is reported that the small size of the PVP-synthesized Pd nanoparticles, suggesting much smaller activation energy for CO oxidation on Pd/alumina (Stara et al. 1995). Above characterization results (TEM results) confirm the well-established fact that small Pd nanoparticles with narrow size distribution supported on Al_2O_3 with high BET surface area are active for low-temperature CO oxidation (Qu et al. 2014). The particle size of supported Pd catalysts obtained from TEM analysis is fairly in agreement with the particle size obtained from CO chemisorption results.

Activity data

Activity test for ozone decomposition

Ozone decomposition studies are carried on Pd catalysts at various temperatures and are displayed in Fig. 5a. Ozone decomposition studies clearly show that O_3 decomposition is accelerated by temperature. It indicates that activity of Pd-supported catalysts investigated in this study is high enough for O_3 decomposition at low temperature. The blank test (in the absence of any catalyst) results indicate that gaseous O_3 decomposition varied from 17 to 30 % when increasing the temperature from 30 to 120 °C. These results are in agreement with the observation reported by Konova et al. (2004). Ozone decomposition on Al_2O_3 and SiO_2 supports varied from 20 to 46 % on Al_2O_3 and SiO_2 in the temperature range of 30–120 °C. The higher catalytic activity of alumina support may be due to the acidic nature. However, in the presence of supported Pd catalysts, the decomposition of O_3 increased significantly at low temperature. Alumina-supported Pd catalyst showed maximum ozone decomposition compared to the SiO_2-

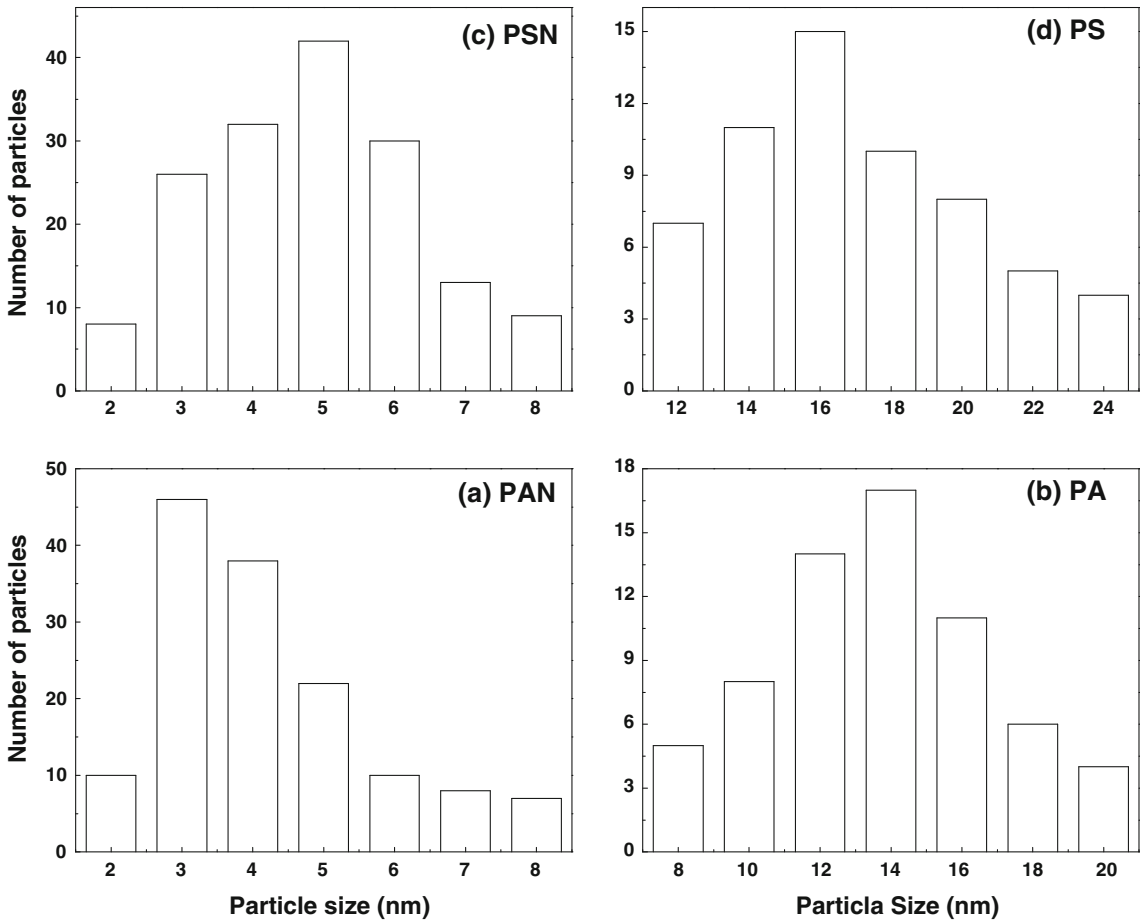

Fig. 4 Histogram of the particle size distributions as calculated from the TEM images. **a** PAN, **b** PA, **c** PSN, **d** PS

supported Pd catalysts at various temperatures (Li and Oyama 1998).

Ozone decomposition with temperature over PA and PAN catalyst varies from 48–85 to 58–90 %, respectively. Whereas, on PS and PSN catalyst, it varies from 29–60 to 36–73 %, respectively. Li and Oyama (2000) have proposed that the adsorbed oxygen species, i.e., peroxide species (O_2^{2-}) and atomic oxygen species (O^-) are formed during the ozone decomposition mechanism on catalysts surface. The reaction is determined to consist of dissociative adsorption of ozone to form an oxygen molecule and an atomic oxygen species, reaction of the atomic species with gaseous ozone molecule to form an adsorbed peroxide species and gas phase oxygen, and decomposition of the peroxide intermediate and desorption of molecular oxygen.

Effect of temperature

Figure 5b shows the effect of reaction temperature on CO conversion for Pd/Al_2O_3 and Pd/SiO_2 supported impregnated and PVP synthesized nanocatalyst. It should be noted that CO conversion in the presence of air (less than 30 % at temperatures below 120 °C) is observed for impregnated catalyst (not shown in figure). The gas phase ozonation of CO is varied from 11 to 46 % in the temperature range of 30–120 °C. With increase in reaction temperature, the CO conversion values increased and the CO conversion is higher in presence of ozone compared to that of air. However, it is interesting to observe that when both O_3 and catalyst are employed in CO oxidation reaction, the PVP-synthesized Pd catalyst shows a dramatic change in CO conversion compared to the impregnated catalysts. The CO conversion is observed to be 56 % at 50 °C and increased with increase in reaction temperature and complete CO conversion achieved above at 80 °C over the PAN catalyst, as shown in Fig. 5b. This temperature is lower than that of the PA catalyst over which the CO conversion is 40 % at 30 °C and reaching almost 90 % at 120 °C. Alumina-supported Pd catalysts prepared by polyol and impregnation method showed higher CO conversion values as compared to silica-supported catalysts. Carbon monoxide conversion is higher on PSN catalyst (increasing from 34 to 84 %) in the reaction temperature range of 30–120 °C, whereas in case of PS catalyst the conversion values increased from 20 to 72 %.

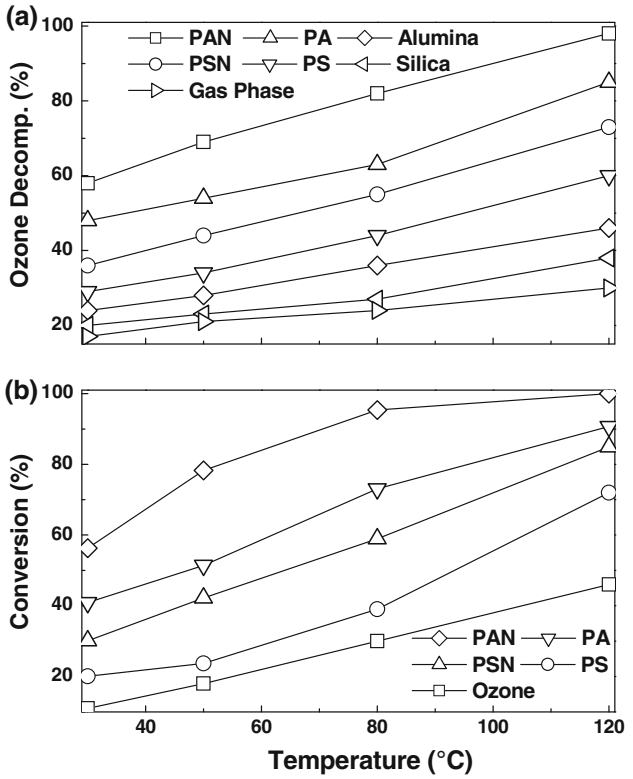

Fig. 5 Effect of reaction temperature on **a** ozone decomposition at contact time = 0.8 s; O_3 = 1600 ppmv. **b** CO oxidation on reduced Pd/Al_2O_3 and Pd/SiO_2 catalysts in various reaction conditions at contact time = 0.8 s; O_3/CO = 3.5

In present study, the results clearly related to the ozone decomposition study at various temperatures. No deactivation of the Pd/SiO_2 and Pd/Al_2O_3 catalysts are observed even though the reaction temperature is raised to 120 °C. Even though the catalysts have similar amounts of Pd, enhanced catalytic activities have been observed for the CO oxidation reaction due to the small crystal sizes with narrow size distribution of Pd nanoparticles over PAN nanocatalyst. The highly dispersed nanoparticles of palladium species as a result of increasing decomposition of ozone may be the reason for the low temperature activity for CO oxidation over PAN nanocatalysts. Shen et al. (2011) reported that for Pd-Cu-Cl_x/Al_2O_3 catalyst which is utilized for CO oxidation process, Pd is the main catalytic active phase in synthesized nanocatalyst. Meyer et al. (2004) reported that the CO oxidation reaction occurs at the particle/oxide interface and exhibits a particle size effect. The smaller particles produce more CO_2 which confirmed that the CO conversion strongly depends on the Pd particles size. Garbowski et al. (1994) attributed the activation of Pd/Al_2O_3 to structural changes from Pd (111) to Pd (200) occurring in the presence of the reactive mixture that facilitates the change from oxidized Pd to reduced Pd. Yang et al. (2000) have shown that during reaction, the Pd surface of a Pd/ZrO_2 catalyst undergoes a transformation to a very active phase consisting of Pd/PdO_x. Baumer and Freund (1999) reported that carbon deposition is never detected on CO-exposed Pd particles deposited on alumina support by photoelectron spectroscopy. The silica supported catalysts exhibited low catalytic activity for CO oxidation. Thus the difference in catalytic activities in the two support systems reported in this paper may be ascribed to a size effect. This result shows that the catalyst-support interaction is not really important in determining its activity, as far as silica support is concerned when ozone employed as an oxidant.

Effect of contact time

CO conversions as a function of contact time over Pd/Al_2O_3 and Pd/SiO_2 catalysts in presence of ozone are studied at 80 °C (Fig. 6a). The contact time varied from 0.2 to 1.2 s at O_3/CO ratio 3.5. The influence of contact time is more significant at higher reaction temperature. In the presence of PAN catalyst, with increasing contact time from 0.2 to 0.6 s the conversion value of CO increased from 56 to 74 %. Further increasing the contact time shows a dramatic change in CO conversion value reaching above 95 % at 0.8 s and holding at 100 % till 1.2 s; while in the case of PA catalyst, CO conversion is observed up to 40 % at 0.2 s and almost attaining a maximum value of 90 % at 1.2 s. On the other hand, the conversion values increase from 34 to 78 % for PSN catalyst and from 22 to 57 % for PS catalyst with increase in contact time. Alumina-supported catalysts are found to be showing higher CO conversion compared to the silica-supported catalysts under comparable conditions. This might indicated that the enough contact time making the fast diffusion of gas reactants to the catalyst surface, resulting in the higher CO conversion. This result supports the experimental observations that the effectiveness of ozone for carbon monoxide oxidation is higher at maximum contact time.

Effect of ozone to CO molar ratios

In order to ascertain the effect of ozone concentration on the CO conversion for Pd-supported catalysts, a set of experiments are conducted by varying ozone/CO mole ratios from 2.5 to 4.5 at 80 °C and the results are shown in Fig. 6b. It is observed that CO conversion at these elevated temperature increases almost linearly with increase in ozone/CO mole ratio. The CO conversion is observed to be 74 % at 2.5 ozone/CO ratio and increased with increase in ozone/CO ratio. The complete CO conversion occurred above ozone/CO ratio of 3.5 over PAN catalyst compared to PA catalyst and attained maximum of 91 %. In the presence of PSN catalyst, with increasing ozone/CO ratio

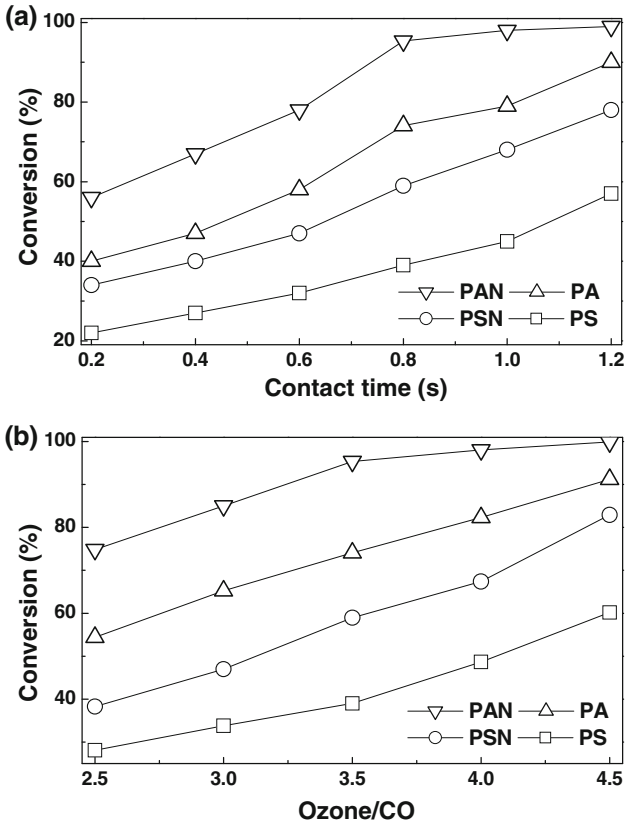

Fig. 6 **a** Effect of contact time on CO oxidation over reduced Pd/Al_2O_3 and Pd/SiO_2 conventional and nanocatalyst at O_3/CO mole ratio 3.5; Temp = 80 °C. **b** Effect of O_3/CO molar ratio on the oxidation of CO over reduced Pd/Al_2O_3 and Pd/SiO_2 catalyst at contact time 0.8 s; Temp = 80°C

from 0.7 to 2.5, CO conversion is increased from 38 to 82 %. In the presence of PS catalyst, an increase from 28 to 60 % is observed. It is clear from the results that as ozone concentration increases, formation of O_2^{2-} oxidants on the catalyst surface increases and this accelerates the carbon monoxide oxidation in addition to the enhanced ER mechanism (Almquist et al. 2007). The obtained results showed that the synthesized nanocatalyst has good performance even at higher concentrations of CO.

Time on stream study

Time on stream analysis over Pd/Al_2O_3 and Pd/SiO_2 catalysts are studied during CO oxidation at 120 °C (Fig. 7). The initial conversion is almost 100 % over PAN catalyst and exhibits a complete conversion of CO; it does not much change with time. Rather, PA catalyst activity decreased slightly from 90 to 86 %. The relatively high conversion in CO oxidation on PAN catalyst may be due to the small size of Pd nanoparticles compared to PA catalyst. The initial conversion is about 85 % over PSN catalyst and

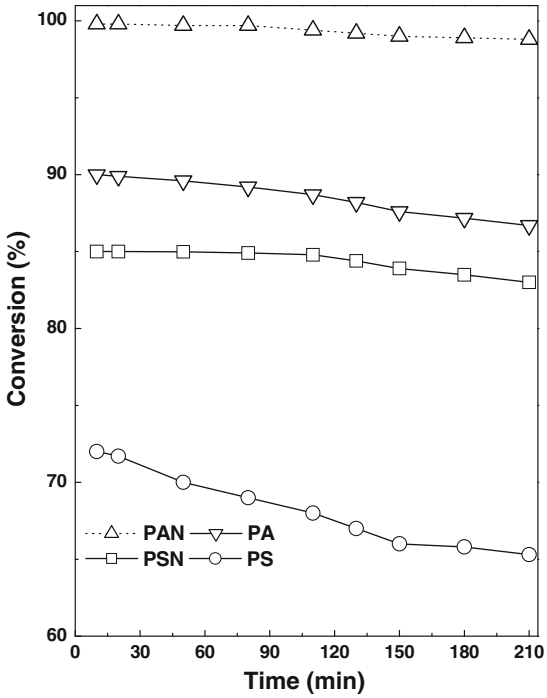

Fig. 7 Time on stream study at 120 °C, O_3/CO mole ratio = 3.5 and contact time = 1.2 s

the conversion values attained a stable value (83 %) in 2 h. The activity obtained after 2 h is ascribed to the steady-state conversion. In contrast, the conversion values for PS catalyst decrease from 72 to 65 % with increasing reaction time. The decrease in CO conversion over impregnated catalyst indicates that a fraction of the active sites may be deactivated and unable to convert the ozone in active species. The smaller Pd nanoparticles, minimized the deactivation of Pd surface besides steady state achieved much faster compared to that of conventional Pd catalysts. The time on stream analysis data reveals that PAN catalyst attained the steady state much faster which implies that relatively the reconstitution of Pd is minimum in case of PAN catalyst.

It is suggested that the catalytic reaction of CO and ozone involves the decomposition of ozone on site to produce a free O_2 molecule and a surface oxygen atom (Oyama 2000; Naydenov et al. 1995). The CO oxidation over Pd catalysts, CO firstly adsorbed on the Pd^0 species then the adsorbed CO reacted with the Pd^{2+}–O species to produce CO_2 and Pd^0. The Pd^0 would be replenished by O_3 to form the new active oxygen species and complete the redox cycle. This means that decomposition of ozone precedes the oxidation of CO, so the ER mechanism is possible (Mehandjiev et al. 2001; Soni et al. 2014). The small size of Pd nanoparticles enhances the CO oxidation in the presence of ozone. The synergistic effect of Pd nanoparticles and ozone enhanced re-oxidation (Pd^{2+} ↔

Pd^0) of palladium species which are responsible for the low-temperature CO oxidation. Therefore, the small size of Pd nanoparticles and the activation of gaseous ozone played an important role in the CO oxidation at lower temperatures. It is considered that well dispersed Pd nanoparticles would weaken C–O and O–O bonds after CO and O_2 adsorption and influence the interaction between the surface and the adsorbents and favoring CO activation (Liu et al. 2012). Initially, CO adsorption takes place strongly and almost exclusively on palladium (Pd^0) active sites and CO coverage is higher on palladium catalyst, resulting in no active sites for ozone activation at low temperature. With increasing temperature or ozone concentration, Pd sites become available for ozone decomposition, which can then offer active oxygen species for CO oxidation (Petersson et al. 2006).

Conclusion

For the purpose of catalytic CO oxidation, the supported Al_2O_3 and SiO_2 palladium nanoparticles are prepared using polyol method and impregnation method. The minimum reduction of BET surface areas and shifting of mesopore are also observed for PVP-synthesized catalysts, compared to the impregnated catalysts. TPR results confirmed that presence of smaller particles and higher Pd dispersion in the PVP-synthesized catalyst, which is due to small peak area of β-PdH_x. TEM results indicate that Pd particle size of PVP-synthesized catalysts become much smaller (from 2 to 8 nm) compared with impregnated samples (from 11 to 24 nm). The results of XRD, CO uptake and TEM show that Pd species are highly dispersed on Al_2O_3 support compared to the SiO_2 by using PVP as a stabilizer. The results demonstrated that PVP-synthesized Pd/Al_2O_3 nanocatalyst is more efficient among the catalysts under comparable conditions, due to the smallest size of Pd (3 nm) and the highest ozone decomposition. CO oxidation increased linearly with temperature and complete conversion achieved at 80 °C over Pd/Al_2O_3 nanocatalyst. CO conversion is observed above 95 % over PVP-synthesized Pd/Al_2O_3 catalyst during the long time stability test, while 65 % conversion is maintained over Pd/Al_2O_3-impregnated catalyst.

Acknowledgments The author would like to thank Dr KS Rama Rao, IICT, Hyderabad and Dr GK Prasad, Scientist, DRDE, Gwalior. One of the authors (KS) is grateful to the JECRC University, Jaipur, and Defence Research and Development Organization, Delhi, India, for the partial support of this study.

References

Almquist CB, Sahle-Demessie E, Sehker SC, Sowash J (2007) Methanol oxidation using ozone on titania-supported vanadia catalyst. Environ Sci Technol 41:4754–4760

Babu NS, Lingaiah N, Gopinath R, Reddy PSS, Sai Prasad PS (2007) Characterization and reactivity of alumina-supported pd catalysts for the room-temperature hydrodechlorination of chlorobenzene. J Phys Chem C 111:6447–6453

Baumer M, Freund HJ (1999) Metal deposits on well-ordered oxide films. Prog Surf Sci 61:127–198

Berger D, Traistaru GA, Vasile BS, Jitaru I, Matei C (2010) Palladium nanoparticles synthesis with controlled morphology obtained by polyol method. UPB Sci Bull Ser B 72:113–120

Bumajdad A, Zaki MI, Eastoe J, Pasupulety L (2006) Characterization of nano-cerias synthesized in microemulsions by N_2 sorptiometry and electron microscopy. J Colloid Interface Sci 302:501–508

Chandra Shekar S, Krishna Murthy J, Kanta Rao P, Rama Rao KS (2003) Selective hydrogenolysis of dichlorodifluoromethane on carbon covered alumina supported palladium catalyst. J Mol Catal A Chem 191:45–59

Chang CL, Sheng LT (2005) Pt/Rh and Pd/Rh catalysts used for ozone decomposition and simultaneous elimination of ozone and carbon monoxide. React Kinet Catal Lett 86:91–98

Chou KS, Chen CC (2007) Fabrication and characterization of silver core and porous silica shell nanocomposite particles. Microporous Mesoporous Mater 98:208–213

Estifaee P, Haghighi M, Mohammadi N, Rahmani F (2013) CO oxidation over sonochemically synthesized Pd–Cu/Al_2O_3 nanocatalyst used in hydrogen purification: effect of Pd loading and ultrasound irradiation time. Ultrason Sonochem 21:1155–1165

Gadgil MM, Sasikala R, Kulshreshtha SK (1994) CO oxidation over Pd/SnO_2 catalyst. J Mol Catal 87:297–309

Garbowski E, Feumi-Jantou C, Mouaddib N, Primet M (1994) Catalytic combustion of methane over palladium supported on alumina catalysts: evidence for reconstruction of particles. Appl Catal A Gen 109:277–291

Gunay ME, Yildirim R (2013) Modeling preferential CO oxidation over promoted Au/Al_2O_3 catalysts using decision trees and modular neural networks. Chem Eng Res Des 91:874–882

Hao Z, Cheng D, Guo Y, Liang Y (2001) Supported gold catalysts used for ozone decomposition and simultaneous elimination of ozone and carbon monoxide at ambient temperature. Appl Catal B Environ 33:217–222

Haruta M, Date M (2001) Advances in the catalysis of Au nanoparticles. Appl Catal A Gen 222:427–437

Haruta M, Tsubota S, Kobayashi T, Kageyama H, Genet MJ, Delmon B (1993) Low-temperature oxidation of CO over gold supported on TiO_2, Fe_2O_3, and Co_3O_4. J Catal 144:175–192

Heck RM, Farrauto RJ (2002) Catalytic air pollution control: commercial technology, 2nd edn. Wiley, New York, pp 69–129

Hirai H, Chawaya H, Toshima N (1985) Colloidal palladium protected with poly(*N*-vinyl-2-pyrrolidone) for selective hydrogenation of cyclopentadiene. React Polym 3:127–141

Huang HH, Ni XP, Loy GL, Chew C, Tan KL, Loh FC, Deng JF, Xu GQ (1996) Photochemical formation of silver nanoparticles in poly (*N*-vinylpyrrolidone). Langmuir 12:909–912

Konova P, Naydenov A, Tabakova T, Mehandjiev D (2004) Deactivation of nanosize gold supported on zirconia in CO oxidation. Catal Com 5:537–542

Kugai J, Moriya T, Seino S, Nakagawa T, Ohkubo Y, Nitani H, Yamamoto TA (2013) Comparison of structure and catalytic performance of Pt–Co and Pt–Cu bimetallic catalysts supported on Al_2O_3 and CeO_2 synthesized by electron beam irradiation

method for preferential CO oxidation. Int J Hydrog Energy 38:4456–4465
Kulshreshtha SK, Gadgil MM (1997) Physico–chemical characteristics and CO oxidation studies over Pd/(Mn_2O_3+SnO_2) catalyst. Appl Catal B Environ 11:291–305
Lashina EA, Slavinskaya EM, Chumakova NA, Stonkus OA, Gulyaev RV, Stadnichenko AI, Chumakov GA, Boronin AI, Demidenko GV (2012) Self–sustained oscillations in CO oxidation reaction on PdO/Al_2O_3 catalyst. Chem Eng Sci 83:149–158
Li W, Oyama ST (1998) Mechanism of ozone decomposition on a manganese oxide catalyst. 2. Steady-state and transient kinetic studies. J Am Chem Soc 120:9047–9052
Li S, Liu G, Lian H, Jia M, Zhao G, Jiang D, Zhang W (2008) Low–temperature CO oxidation over supported Pt catalysts prepared by colloid-deposition method. Catal Com 9:1045–1049
Lim B, Xiong Y, Xia Y (2007) A water-based synthesis of octahedral, decahedral, and icosahedral Pd nanocrystals. Angew Chem Int Ed 46:9279–9282
Liu L, Qiao B, He Y, Zhou F, Yang B, Deng Y (2012) Catalytic co-oxidation of CO and H_2 over FeO_x–supported Pd catalyst at low temperatures. J Catal 294:29–36
Lu P, Teranishi T, Asakura A, Miyake M, Toshima N (1999) Polymer-protected Ni/Pd bimetallic nano-clusters: preparation, characterization and catalysis for hydrogenation of nitrobenzene. J Phys Chem B 103:9673–9682
Mehandjiev D, Naydenov A, Ivanov G (2001) Ozone decomposition, benzene and CO oxidation over $NiMnO_3$-ilmenite and $NiMn_2O_4$-spinel catalysts. Appl Catal A Gen 206:13–18
Meyer R, Shaikhutdinov SK, Freund HJ (2004) CO oxidation on a Pd/Fe_3O_4 (111) model catalyst. Z Phys Chem 218:905–914
Mulvaney P (1996) Surface plasmon spectroscopy of nanosized metal particles. Langmuir 12:788–800
Naccache C (1971) ESR study of species formed by reaction of O^-, adsorbed on magnesium oxide with O_2, CO and ethylene. Chem Phys Lett 11:323–325
Nadgeri JM, Telkar MM, Rode CV (2008) Hydrogenation activity and selectivity behavior of supported palladium nanoparticles. Catal Com 9:441–446
Naydenov A, Stoyanova R, Mehandjiev D (1995) Ozone decomposition and CO oxidation on CeO_2. J Mol Catal A Chem 98:9–14
Oyama ST (2000) Chemical and catalytic properties of ozone. Catal Rev Sci Eng 42:279–322
Padmasri AH, Venugopal A, Krishnamurthy J, Rama Rao KS, Kanta Rao P (2002) Novel calcined Mg–Cr hydrotalcite supported Pd catalysts for the hydrogenolysis of CCl_2F_2. J Mol Catal A Chem 181:73–80
Petersson M, Jonsson D, Persson H, Cruise N, Andersson B (2006) Ozone promoted carbon monoxide oxidation on platinum/γ–alumina catalyst. J Catal 238:321–329
Qu Z, Zhang X, Yu F, Jia JA (2014) Simple one pot synthesis of mesoporous silica hosted silver catalyst and its low-temperature CO oxidation. Microporous Mesoporous Mater 188:1–7
Richard Y (1993) Use of ozone and flotation for the treatment of a reservoir water: the dinan case history. Ozone Sci Eng 15:465–480
Sarkar A, Kapoor S, Mukherjee T (2005) Preparation, characterization, and surface modification of silver nanoparticles in formamide. J Phys Chem B 109:7698–7704
Seyfi B, Baghalha M, Kazemian H (2009) Modified $LaCoO_3$ nano-perovskite catalysts for the environmental application of automotive CO oxidation. Chem Eng J 148:306–311
Shen Q, Min Q, Shi J, Jiang L, Zhang JR, Hou W, Zhu JJ (2009) Morphology-controlled synthesis of palladium nanostructures by sonoelectrochemical method and their application in direct alcohol oxidation. J Phys Chem C 113:1267–1273
Shen Y, Lu G, Guo Y, Wang Y, Guo Y, Gong X (2011) Study on the catalytic reaction mechanism of low temperature oxidation of CO over Pd–Cu–Cl_x/Al_2O_3 catalyst. Catal Today 175:558–567
Simonov PA, Romanenko AV, Prosvirin IP, Moroz EM, Boronin AI, Chuvilin AL, Likholobov VA (1997) On the nature of the interaction of H_2PdCl_4 with the surface of graphite–like carbon materials. Carbon 35:73–82
Soni K, Chandra Shekar S, Singh B, Agrawal A (2014) Catalytic oxidation of CO in presence of ozone over supported palladium catalysts. Indian J Chem Sect A 53:484–492
Soni KC, Shekar SC, Singh B, Gopi T (2015) Catalytic activity of Fe/ZrO_2 nanoparticles for dimethyl sulfide oxidation. J Colloid Interface Sci 446:226–236
Stara I, Nehasil V, Matolin V (1995) The influence of particle size on CO oxidation on Pd/alumina model catalyst. Surf Sci 33:173–177
Telkar MM, Rode CV, Chaudhari RV, Joshi SS, Nalawade AM (2004) Shape-controlled preparation and catalytic activity of metal nanoparticles for hydrogenation of 2-butyne-1,4-diol and styrene oxide. Appl Catal A Gen 273:11–19
Toebes ML, van Dillen JA, de Jong KP (2001) Synthesis of supported palladium catalysts. J Mol Catal A Chem 173:75–98
Wang F, Xu Y, Zhao K, He D (2014) Preparation of palladium supported on ferric oxide nano-catalysts for carbon monoxide oxidation in low temperature. Nano Micro Lett 6:233–241
Weiliang H, Peng Z, Xia P, Zhicheng T, Gongxuan L (2013) Highly active Pd/Fe based catalyst prepared with polyol-reduction method for low-temperature CO oxidation. J Environ Chem Eng 1:189–193
Yang S, Maroto-Valiente A, Benito-Gonzalez M, Rodriguez-Ramos Y, Guerrero-Ruiz A (2000) Methane combustion over supported palladium catalysts: I. Reactivity and active phase. Appl Catal B Environ 28:223–233
Yu J, Wu G, Mao D, Lu GZ (2008) Effect of La_2O_3 on catalytic performance of Au/TiO_2 for CO oxidation. Acta Phys Chim Sin 24:1751–1755
Yu J, Wu GS, Mao DS, Lu GZ (2009) Change of the surface species on Au/CeO_2-TiO_2 during in the reduction and CO oxidation. Acta Chim Sin 67:1407–1411